IN-20
58072
p. 23

NASA Technical Memorandum 105143
AIAA-91-2226

High-Power Hydrogen Arcjet Performance

Thomas W. Haag and Francis M. Curran
Lewis Research Center
Cleveland, Ohio

Prepared for the
27th Joint Propulsion Conference
cosponsored by the AIAA, SAE, ASME, and ASEE
Sacramento, California, June 24-27, 1991

NASA

ERRATA

NASA Technical Memorandum 105143
AIAA-91-2226

HIGH-POWER HYDROGEN ARCJET PERFORMANCE

Thomas W. Haag and Francis M. Curran
June 1991

Table III was omitted from page 9 of the original publication. Pages 8 and 9 have been revised to include table III.

HIGH-POWER HYDROGEN ARCJET PERFORMANCE

Thomas W. Haag and Francis M. Curran
National Aeronautics and Space Administration
Lewis Research Center
Cleveland, Ohio 44135

ABSTRACT

A hydrogen arcjet was operated at power levels ranging from 5 to 30 kW with three different nozzle geometries. Test results using all three nozzle geometries are reported and include variations of specific impulse with flow rate, and thrust with power. Geometric variables investigated included constrictor diameter, length, and diverging exit angle. The nozzle with a constrictor diameter of 1.78 mm and divergence angle of 20° was found to give the highest performance. A specific impulse of 1460 s was attained with this nozzle at a thrust efficiency of 29.8%. The best efficiency measured was 34.4% at a specific impulse of 1045 s. Post test examination of the cathode showed erosion after 28 hours of operation to be small, and limited to the conical tip where steady state arc attachment occurred. Each nozzle was tested to destruction.

INTRODUCTION

High power hydrogen arcjets are currently being considered for primary propulsion functions, such as orbit transfer. Development efforts were conducted on hydrogen arcjet thrusters in the early 1960's. The Giannini Scientific Corp. produced a 30 kW hydrogen arcjet during this period.[1] The design made extensive use of regenerative heat transfer, whereby incoming propellant was preheated within the thruster body and nozzle walls before injection into the arc. The design also included a mixing chamber anode attachment region immediately upstream of a diverging nozzle. This was an effort to promote recombination of dissociated gas molecules to reduce frozen flow losses. At 30 kW, thrust efficiencies as high as 55% were reported at a specific impulse of 1000 s.

The Avco Corporation was also involved in a similar development program for 30 kW class hydrogen arcjet thrusters.[2] Their design employed a conventional cylindrical constrictor and placed less emphasis on regenerative heat transfer. The result was a thruster with a greater tolerance for heat loads, which was able to run at substantially higher power to mass flow rates (specific powers) than the Giannini concept. Specific impulses as high as 1530 s were claimed, at thrust efficiencies of about 45%.

Due to the lack of large space power systems, there has been little effort on concepts for primary electric propulsion until recently. Some efforts have been conducted on 30 kW arcjets for use with ammonia,[3] although there is a fundamental specific impulse penalty when compared to lighter molecular weight propellants. The high performance of hydrogen arcjet propulsion may offer a considerable propellant weight savings over chemical systems for LEO to GEO orbital transfer missions. Such a weight savings may allow the reduction of launch vehicle requirements to the next smaller class rocket. Such promises have renewed interest in hydrogen arcjet systems. The purpose of this work was to obtain preliminary operating experience with high power hydrogen arcjets, and relate performance with 1960's data.

APPARATUS

While the 30 kW arcjet thruster used in this work is of recent design, its basic arrangement resembles that of a 1 kW arcjet thruster used successfully in a 1000 hr life test operating on hydrogen nitrogen gas mixtures.[4]

The arcjet used in these tests was of conventional constricted design, employing a centered cathode electrode and an axisymmetric diverging nozzle anode electrode. The cathode attachment of the arc occurred in a high pressure vortex stabilized flow field upstream of the constrictor. The arc column proceeded down the length of the constrictor and was seated diffusely on the anode end in a low pressure diverging flow field. Three different constrictor-nozzle geometries were investigated, over a wide range of propellant flow rates and arc power levels. Each one was fabricated from 2 % thoriated tungsten and had a 30° convergence angle immediately upstream of the constrictor. The primary variables in nozzle geometry included constrictor diameter, constrictor length, and downstream divergence angle.

Nozzle A (Fig. 1(a)) had a 2.54 mm diameter constrictor which was 5.08 mm in length, for a ℓ/d ratio of 2. A 20 degree diverging nozzle ended at an exit diameter of 24.3 mm, resulting in an expansion area ratio of 88 : 1.

The emphasis for nozzle B (Fig. 1(b)) was to maximize the area ratio. It had a 1.78 mm diameter constrictor which was 3.56 mm in length, and a ℓ/d ratio of 2. This nozzle had a divergence angle of 20° but ended with an exit diameter of 29 mm. Due to the larger exit diameter and smaller constrictor diameter it had a considerably larger area ratio of 270 : 1.

Nozzle C (Fig. 1(c)) had a 2.54 mm diameter constrictor, as in nozzle A, but with a length of only 0.71 mm. A narrower divergence angle of 10 degrees was used. The exit diameter was 24.3 mm as in nozzle A, and had an area ratio of 88 : 1.

The same cathode was used in all tests. It consisted of a 2% thoriated tungsten rod 6.35 mm in diameter and approximately 30 cm in length. A 30 degree conical tip was machined on the end at which arc attachment was to occur. The arc gap was set by pushing the cathode rod in until it touched the anode, and then withdrawing it by 1.27 mm.

A vortex chamber cavity 16 mm in diameter surrounded the cathode tip immediately upstream of the constrictor. Four propellant injection holes 0.89 mm in diameter admitted hydrogen gas tangentially into this chamber to establish a high strength vortex flow field around the arc column.

A heavy walled anode housing held the nozzle, propellant injector, and cathode in alignment during operation (Fig. 2). It also functioned to absorb and dissipate heat deposited into the nozzle walls from the anode arc attachment. In order to enhance heat transfer, the tungsten nozzle was lapped into the anode housing to obtain a very close taper fit between the two parts. A graphite aerosol spray significantly increased the radiant thermal emissivity of the anode surface and was used routinely.

A boron nitride insulator centered the cathode within the anode housing. The insulator contained grooved passages around its perimeter with the anode housing, through which propellant was heated prior to injection into the arc.

The rear assembly of the arcjet thruster performed a variety of functions. A back insulator made of boron nitride contained a modified compression fitting at its rear to serve as a cathode feedthrough. This fitting clamped the cathode rod at a specified arc gap and sealed it against propellant leaks. A propellant feed tube was attached to the back insulator and was tapped into a stainless steel anchor at the center of the insulator. This allowed the propellant tube to be electrically isolated from both cathode and anode potential. A heat resistant inconel spring and boron nitride compression plunger were located in the forward area of the rear assembly. Their function was to keep the entire internal arrangement of the thruster under constant compression, thereby sealing all interior graphite gasket joints.

The anode housing and rear insulator assembly were joined together by a threaded rod and flange arrangement. The flanges were made from 3.8 mm thick molybdenum plate and were designed to flex slightly upon assembly, thus maintaining uniform pressure on this joint, regardless of thermal effects. A graphite gasket located between the anode housing and rear assembly prevented propellant leakage, and was under constant compression from the flanges.

Testing was carried out in a vacuum facility which was 4.6 m in diameter and 20 m in length. The thrust stand was installed in a 0.9 m diameter port extension to the main vacuum tank and could be isolated through a 0.9 m gate valve (Fig. 3). The port extension was perpendicular to the main tank. A pyrolytic graphite target was placed 4 m downstream of the arcjet in order to disperse plume heat and avoid direct impingement on the opposing tank wall. Pumping in this facility was carried out by four rotary blowers yielding a combined capacity of 5.8 m^3/s. These were backed by four 0.24 m^3/s reciprocating pumps which discharged to atmosphere. Depending on propellant flow rate, the ambient background pressure in the facility during tests was between 13 Pa and 53 Pa (0.1 and 0.4 torr).

The arcjet electrical source used in this work was a resistance ballasted power supply with a two stage igniter. (Fig.4) A 75 kW industrial type power supply was used, which had been configured to operate in a current limited mode of control. This unit had an open circuit voltage of 250 V and a current capacity over 300A. An output filter consisting of a 750 uH inductor and a 0.11 F capacitor bank was used to minimize ripple. A 250 uH inductor and ballast resistor limited current surges to the arcjet and allowed the power supply to operate stably into the negative impedance characteristics of the arc discharge. The ballast resistor consisted of a fan cooled arc welder load bank and had selector switches through which a resistance was chosen. A typical resistance was 0.1 ohms.

Since the open circuit voltage of the main power supply was limited to 250 V, a separate high voltage circuit was utilized for arc ignition. Initial breakdown was achieved with a 1200 V igniter, with a steady state current capacity of 0.5 A. The voltage of the arc discharge from the igniter was reduced using an intermediate 600 V, 15 A power supply. The voltage of the 15 A discharge was always within range of the main power supply, which was slowly ramped up to achieve the desired power level. Blocking diodes protected both the 15 A and 300 A units during this starting procedure.

Thrust measurements for these tests were conducted on a calibrated displacement type thrust stand similar in design to thrust stands used with 1 kW arcjets.[5] The

thruster was mounted to a platform which was in turn supported by an upright flexure arrangement. The flexures restricted all motion except for that along an axis parallel to the thrust vector. A rear view of the thrust stand is shown in Figure 5. An interchangeable load spring could be adjusted to match the sensitivity requirements of the test. Thrust induced displacements of up to 5 mm were measured using a linear variable differential transformer (LVDT). Displacement resolution to within 0.001 mm was obtained.

Because flexures provided a frictionless means of thrust stand movement, hysteresis effects amounted to only a fraction of one percent full scale thrust. Displacement oscillations due to transient arc behavior were physically damped out using a derivative feedback loop. Arcjet propellant was supplied through the thrust stand by means of an internal propellant flexure, which was a 4.8 mm stainless steel tube bent into a rectangular shape and anchored to the thrust stand base at its lower end. The upper end was anchored to the mounting platform of the thrust stand so that the entire tube could flex during displacements with relatively little stiffness. Cooling water was routed onto the thrust stand through 3 mm tubes in a similar fashion.

Arc current to the arcjet was sent through the thrust stand using internal electrical flexures, which are shown in the foreground of Figure 5. Two water cooled copper tubes 6 mm in diameter were formed into a rectangular flexure loop and mounted in a plane perpendicular to thrust stand motion. This orientation was chosen so that any thermal expansion would result in radially outward movement of the flexure loop perimeter, and could not be resolved into the sensitive axis of the thrust stand. Resistive heat in the conductors was removed using a temperature controlled water bath, which maintained its temperature to within +/- 1.0 °C. These water cooled tubes conducted both polarities of current, starting at the base and terminating near the thruster mounting platform on the moving part of the thrust stand. The conductors were routed as close together as possible to minimise magnetic coupling with other parts of the installation. Stranded 4/0 cable was used as a jumper for the final connection to the arcjet. All copper tubing and connection fittings were insulated with silicone rubber tape to prevent arcing. Since the hard walled copper tubes were all that would flex during thrust stand motion, there were no frictional tares as would be present with stranded cable.

A water cooled copper enclosure (not shown in Figure 5) surrounded the entire thrust stand to prevent radiant heat from impinging on the flexures and structural components. A water cooled thruster mounting column and electrical power connections were all that protruded from this enclosure.

In-situ calibration of the thrust stand was performed using three 100 g masses. The masses could be lowered in succession, and would engage the thrust stand through a monofilament nylon line which passed over a precision pulley. A rotary vacuum feedthrough was used to manually lower each mass, which could be done at any time during a series of tests.

A +/-10 volt analog signal was output by the LVDT readout and used as a thrust signal. This was routed to the oscillation damping circuit and a strip chart recorder to provide a permanent record of test operations.

Due to the low thrust to weight ratio of the arcjet, thrust measurements were very sensitive to angular tilting and distortions of the vacuum facility. Thermal radiation absorbed by the test port walls resulted in such deviations and would manifest itself in the form of thermal drift. Such deviations were monitored with an angular inclinometer mounted on the thrust stand base and could be compensated for using a leveling mechanism. Remote control leveling of the thrust stand to a resolution of 10 seconds of arc was possible.

A thrust stand verification test was conducted during the facility buildup to determine if magnetic fields induced by the arc current would interfere with thrust measurements. The arcjet was temporarily shorted from cathode to anode and installed on the thrust stand. Currents as high as 200 A through the thrust stand electrical flexures had no measurable effects on the neutral thrust signal.

During normal arcjet testing, an electrically isolated digital voltmeter was used to measure arc voltage with a resolution of 0.1 V. This unit was checked periodically to verify its integrity. Arc current was measured using a 500 A, 50 mV shunt connected to an isolated voltmeter, which provided a resolution of 0.1 amp.

Propellant flow rates were measured and regulated with a 0-200 slpm flow controller and digital readout. Ultra high purity (99.999%) gaseous hydrogen was used for all arcjet operation in these tests. The hydrogen was stored in high pressure bottles and regulated to 1.03 MPa where it entered the flow controller. An electrical interlock circuit disabled the arc power supply if the hydrogen bottle pressure dropped below 620 KPa. The hydrogen flow controller was calibrated in-situ to ensure accurate mass flow measurements.

Propellant pressure was measured through a pressure tap located in the propellant feed tube 15 cm upstream of the arcjet. This pressure tap was fed through the thrust stand to a digital transducer located outside the vacuum tank. While feed pressure measurements were recorded, they were mainly used for diagnostic purposes.

Ambient background pressure within the vacuum facility was monitored using a capacitance manometer type transducer and displayed on a digital readout. The sensor

head was attached directly to the 0.9 m test port, in the vicinity of the arcjet thruster.

A two color pyrometer was used to observe arcjet nozzle temperature during tests. Depending on the specific unit being used, the pyrometer had a range of 900 °C to 1600 °C , or 1400 °C to 2600 °C. While nozzle temperatures were recorded, they were mainly used for thruster health monitoring.

EXPERIMENTAL PROCEDURE

Testing began with cold flow thrust measurements to verify the operation of the facility and instrumentation. This also provided information needed to determine arcjet efficiency. The hydrogen flow controller was set to a specified flow rate and was allowed to equilibrate for at least 1 minute before measurement validity was assumed.

Arc ignition was accomplished in stages due to the limited current and voltage capabilities of the available power supplies. The high voltage igniter was ramped up and breakdown usually occurred between 600-800 volts. This would establish a steady discharge of about 0.5 A at 300-400 V. The intermediate power supply was then turned on and a discharge of 12 A at approximately 150-200 V was established. The igniter power supply was then turned off and the main power supply was manually ramped up to approximately 100 A. The intermediate power supply could be turned off and the main supply adjusted to the correct arc discharge power.

The arc input power was specifically coordinated with the propellant flow rate to establish discrete specific powers of 150, 200, 250, and 300 MJ/kg. The objective was to observe trends in specific impulse and thrust efficiency as the arcjet was throttled in power while maintaining the same specific power level. Each of the three nozzles were operated at similar power and propellant flow rates so that the effects of nozzle geometry could be compared. Once the original test matrix was completed, further exploration at higher power levels was performed and specific powers of up to 340 MJ/kg were eventually reached.

The thruster was allowed to run for at least 10 minutes at set point conditions before final thrust measurements were made, allowing thermal equilibrium to be established (Fig. 6). After a final data set had been taken the arc was extinguished, however propellant was allowed to flow for about 10 seconds so that regenerative thrust power could be determined. When the propellant flow had been shut off an updated thrust zero was established by which the previous thrust measurement was to be referenced. Zero drift was usually not more than a few percent of the measured value.

Cycling of the thrust stand calibration weights was regularly performed within 2 minutes of every test run. Changes in thrust stand sensitivity were usually less than 0.1 % over the course of any test session.

RESULTS AND DISCUSSION

Nozzle A

Nozzle A was the first anode geometry tested. A listing of all data can be found in Table I. Most of the data obtained with this nozzle were at specific powers of 214, 250, 300, and 340 MJ/kg. Arc current was adjusted to establish the appropriate input power level at a given propellant flow rate. Flow rates ranged from a minimum of 30.9 mg/s to a maximum of 182 mg/s.

The temperature of the tungsten nozzle was found to be influenced more by specific power than by input power alone. In spite of a closely lapped joint between the large molybdenum anode housing and tungsten nozzle insert, thermal contact resistance was high enough to allow temperature differences on the order of 500 °C between the two components. The tungsten nozzle temperature was a critical factor which limited input power, and consequently placed an upper bound on attainable specific impulse. Exceeding this limit invariably resulted in metal being ejected from the nozzle. Initial operation began at a nominal power of 15 kW and progressed outward to both lower and higher power levels, with the high risk operating points being performed last.

A plot of arc voltage as a function of arc current is shown in Figure 7 for each propellant flow rate used with nozzle A. Voltage increased from a minimum of 96 V at a flow rate of 31 mg/s, to a maximum of 155 V at 182 mg/s. The lowest current for a given flow rate was determined by the power needed to establish the lowest specific power of 214 MJ/kg. The highest currents were limited by maximum power level or concern for the integrity of the thruster. The voltage levels measured were typically 20% higher than those commonly seen with ammonia propellant.[3] The voltage current curves in Figure 7 represent data accumulated over a time period during which electrode burn-in[6] occurred, resulting in some nonrepeatability in the data.

Figure 8 shows a plot of specific impulse as a function of flow rate with nozzle A, for the specific powers listed earlier. As can be seen, specific impulse increases with increasing specific power, to a maximum of 1411 s obtained at 340 MJ/kg. This data point was acquired late in the test matrix and represents the highest specific power attempted due to nozzle damage which resulted. The maximum flow rate at which the arcjet could be operated was determined by power supply limitations at low specific powers, or the thruster nozzle temperature at high specific powers. The lowest flow rate at which data could be taken was determined by the stability of the arc. At very low

flow rates the exhaust plume diverged from the center thruster axis by a shallow angle, and would wander in random directions during brief periods of arc instability. The arc voltage and thrust would typically decrease by a few percent during such activity, but returned to its previous value as stability resumed. At the highest specific powers these periods of instability appeared to cause nozzle constrictor damage, for it was noticed that small sparks were occasionally expelled during such transient activity.

Specific impulses at minimum flow rates were poor. This characteristic is typical of most arcjet thrusters and recent findings indicate that higher anode fall losses at low flow rates may be responsible for degraded performance.[7,8] At higher flow rates, the pressure in the diverging nozzle is also higher and anode losses decrease. As the propellant flow rate for nozzle A was increased, the specific impulse at a constant specific power increased until a flow rate of about 91 mg/s was reached, after which the specific impulse decreased slightly for the cases where higher flows were achieved. While the increase in specific impulse with flow rate was expected, the decrease as flow rates exceeded 91 mg/s was not. Past experience has been that specific impulse would typically increase and eventually level off as flow rates increase. This unexpected characteristic was seen for most of the flow rates at constant specific power for nozzle A as well as the other two nozzles which are described in following sections. Since back pressure in the vacuum facility increased roughly linearly with flow rate, it is believed that this degradation was caused by high ambient pressure interacting with the arcjet exhaust. This topic goes beyond the intended scope of this work, however this issue is discussed elsewhere.[7,8] It should be pointed out that all data presented has not been corrected for background pressure effects, and therefore are felt to represent conservative performance.

A plot of thrust efficiency as a function of specific impulse can be seen in Figure 9 for a variety of propellant flow rates. Specific impulses obtained with nozzle A ranged from a low of 1028 s to a high of 1411 s. This compares favorably with arcjet performance often obtained with ammonia, which typically ranges from 500 s to 900 s, at roughly the same efficiency. The lowest thrust efficiencies occurred at the lowest propellant flow rates, where arc stability was marginal. Efficiency increased with flow rate to a maximum at about 91 mg/s. The performance then decreased slightly at higher flow rates, corresponding to the decrease in specific impulse seen in Figure 8. The lowest specific impulse for each flow rate occurred at a specific power of 214 MJ/kg. The highest efficiency at any given flow rate often occurred at the lowest specific impulse. The performance of Nozzle A was less than that reported by Avco[2] using hydrogen propellant. At a specific power of 250 MJ/kg, nozzle A achieved 1131 s at an efficiency of 30.1%. Avco reported a specific impulse of 1530 s and an efficiency of 44% in which the thruster was operated at a specific power of 252 MJ/kg. The immediate reason for the lower performance obtained in this work is not yet known.

A plot of specific impulse as a function of specific power can be seen in Figure 10 for flow rates ranging from 30.9 to 182.2 mg/s. Specific impulse is seen to increase almost linearly with specific power over the span of 214 to 340 MJ/kg. The performance for most of the flow rates overlap fairly closely, with the exception being the two lowest flow rates, which showed lower specific impulses than the majority of the data.

A plot of thrust as a function of input power is shown in Figure 11. Arc power ranged from from a low of 6.7 kW to a maximum of 39.5 kW, which represents a power throttling ratio of 5.9 : 1. The lowest thrust of 0.31 N occurred at the lowest power and flow rate. Thrust increased with power level and with successively higher flow rates up to 2.03 N. Similar throttling ranges have been obtained with 30 kW class ammonia arcjets.[11]

As previously mentioned, the tungsten nozzle was damaged from operation at a specific power of 340 MJ/kg. Post test examination of the nozzle revealed arc damage in the downstream half of the constrictor and localized undercutting at the transition point between constrictor and diverging nozzle. The tungsten surface melted in this area but resolidified farther downstream in the form of elongated beads (Fig 12).

Examination of the cathode revealed little damage. The conical tip had been blunted by the arc attachment and the 30 degree point was replaced by a flat truncation approximately 0.8 mm in diameter. The cathode appeared almost identical to its newly machined condition, with the exception of the tip.

Nozzle B

The major difference between nozzles A and B was a reduction in constrictor diameter and length The cathode rod previously used to test nozzle A was reused in its existing condition.

Testing of nozzle B occurred at specific power of 150, 200, 250, 300, and 340 MJ/kg. A complete listing of data taken with nozzle B can be found in Table II. The propellant feed pressure and arc voltage were, as expected, both higher with this nozzle than with nozzle A under comparable conditions.

Figure 13 shows the current voltage characteristics obtained with nozzle B. Most operating voltages were typically 20 % higher than those measured from nozzle A. As shown, the highest voltage of all tests performed was 181.4 V at a flow rate of 148 mg/s. The lowest voltage that occurred with nozzle B was 120.4 V, at a flow rate of

31 mg/s and arc current of 38 A. This current was lower than any tests with nozzle A, partly because lower specific powers were pursued, but also because higher voltages required less current to achieve the same power level. Improved arc stability as a result of the smaller constrictor made the arcjet easier to control at low flow rates.

As seen in Figure 13, the voltage current characteristics are more orderly for nozzle B than they were for nozzle A. Part of this may be due to the cathode acquiring a more stable shape as it is burned in, but it also may be due to the arc operating with more stability and allowing repeatable performance.

A plot of specific impulse as a function of flow rate is shown in Figure 14 for specific powers ranging from 150 to 340 MJ/kg. Many characteristics of this plot are similar to results from nozzle A. Specific impulses for nozzle B were typically 3% higher than those of nozzle A under comparable conditions. The maximum specific impulse obtained with nozzle B up through a specific power of 300 MJ/kg was 1392 s. The nozzle was briefly examined after this point and found to be free of serious arc damage. A final series of tests was carried out with this nozzle at a specific power of 340 MJ/kg and flow rates of 76.2, 91.5 and 122.8 mg/s in order to explore higher performance. The highest specific impulse of all was 1461 s, which occurred at a flow rate of 122.8 mg/s. Testing with this nozzle was discontinued when the constrictor was damage at the lower of the three flow rates.

Thrust efficiency as a function of specific impulse for nozzle B is plotted in Figure 15. Thrust efficiency for nozzle B was typically more than 2 percentage points higher than that of nozzle A. This improvement was present at low values of specific impulse as well as high values.

The higher performance for nozzle B was most likely due to the smaller constrictor diameter and resulting higher pressure for a given propellant flow rate. Higher gas pressure would cause a higher arc impedance within the constrictor and cathode arc chamber region. Since the arcjet was operated at a fixed power level, the higher voltage discharge permitted lower current to achieve a comparable power level. If anode fall losses are proportional to arc current, then the higher voltage of operation for nozzle B may be responsible for some of the improvement in thruster efficiency over nozzle A. In addition to reduced anode losses, high upstream pressure also affects the arc column within the constrictor. It has been shown that recombination rates improved for hydrogen at higher pressures, and that this process can reduce frozen flow losses.[9]

A plot of specific impulse as a function of specific power is shown in Figure 16. A wider range of specific impulse was covered with nozzle B, as can be seen by the groupings of specific powers from 150 to 340 MJ/kg. While data was acquired in a more orderly arrangement with nozzle B, the general trends were quite similar to those of nozzle A.

Thrust as a function of power is shown in Figure 17. The power levels over which the thruster was throttled covered a wider range for nozzle B than any other nozzle tested. Arc power levels as low as 4.6 kW and as high as 41.9 kW were covered. While the nozzle was at higher risk of arc damage at the extremities, this still represents a throttle ratio of 9.2 : 1. Arcjet thrust ranged from 0.29 N to 1.76 N with nozzle B.

As mentioned above, nozzle B remained relatively free of arc damage up through a specific power of 300 MJ/kg. Operation at higher specific powers resulted in considerable melting in the constrictor region. A post test examination of the nozzle revealed extensive erosion in the downstream half of the constrictor. The upstream half was the original 1.78 mm inner diameter, but the downstream half had opened to 2.28 mm. The cathode, however, was still in very good condition.

Nozzle C

The constrictor diameter for nozzle C was identical to that of nozzle A. The divergence angle was 10 degrees, as opposed to the 20 degree angle for nozzles A and B. This shallower angle is more representative of the 7.5 degree Avco thruster nozzle geometry which was tested in the early 1960's.[2] Propellant flow rates ranged from 45 to as high as 213 mg/s. A complete listing of data obtained with nozzle C can be found in Table III.

The most notable characteristic of this nozzle was its unusually high operating temperature. It was often as much as 800 °C hotter than nozzle B at the same conditions. Because of these high temperatures, the specific power for this nozzle was restricted to 150 and 200 MJ/kg. The maximum nozzle temperature reached 2313 °C, and this was at a specific power of only 200 MJ/kg.

Figure 18 shows various voltage and current operating points for nozzle C. Arc voltages were typically 20 % lower than nozzle A, and over 30 % lower than nozzle B at the same power level. Voltages as low as 91.3 V were encountered even though propellant flow rates never fell below 45.2 mg/s. The low voltages observed were somewhat unexpected because it was originally thought that the narrower expansion angle would resulting in a pressure distribution along the diverging walls which would force the arc farther downstream of the constrictor and result in a higher voltage. A shorter constrictor length was originally chosen in anticipation of a higher voltage and was intended to partially compensate for this.

Figure 19 shows a plot of specific impulse as a function of flow rate for the specific powers described

above. The lowest flow rate attempted was 45.2 mg/s, which resulted in a specific impulse of 886 s. In spite of a specific power of only 150 MJ/kg, the nozzle temperature reached 1599 ^{o}C, and was the coolest of any operating point for this nozzle. In comparison, nozzle B reached this temperature only at specific powers approaching 300 MJ/kg. As flow rates at constant specific power increased, the specific impulse gradually improved but at a lower rate than observed with nozzles A and B. Specific impulse increased until a maximum of 1128 s was reached at a flow rate of 154 mg/s and then declined slightly at higher flow rates. Higher values of specific impulse were acquired at a specific power of 200 MJ/kg, where a maximum value of 1128 s was reached at a flow rate of 154 mg/s. This occurred at a nozzle temperature of 2313 C^{o}, which prohibited pursuit of higher specific impulses.

A relation between thrust efficiency and specific impulse can be seen in Figure 10. Because only two specific power levels were tried, there were only two data points for each flow rate. The maximum thrust efficiency obtained with nozzle C was 32.4 % at a flow rate of 154 mg/s and specific power of 150 MJ/kg. The highest efficiency at a specific power of 200 MJ/kg was 30.1 %, which also occurred at this flow rate.

A plot of specific impulse with specific power for nozzle C is shown in Figure 21. For the two specific powers tried with nozzle C, the highest specific impulses occurred at flow rates of 154 mg/s, and the lowest specific impulse occurred at the lowest flow rate.

Thrust as a function of power is shown in Figure 22. In spite of the restriction on specific power, nozzle C was still throttleable over a range in power from 6.7 kW to 30.8 kW and represents a ratio of about 4.6 : 1. Because of the higher flow rates at which this nozzle was operated, thrust varied from 0.4 to 2.1 N.

The thruster was disassembled after use with nozzle C for a final examination. Even though it operated at very high temperatures, the tungsten anode showed little sign of arc damage. There was a small region downstream of the constrictor where local melting had occurred, but the constrictor itself was undamaged.

The cathode showed no major changes during use with nozzle C. The truncated tip was slightly more concave than before. The remainder of the conical surface displayed a slight sand blasted appearance but its shape had not been significantly altered from the way it was originally machined.

The cathode which had been used for testing all three nozzle geometries had endured 141 starts and accumulated approximately 28 hours of run time. As can be see in Figure 23, aside from a truncated tip, the appearance of the cathode compares quite closely to the way it was prior to testing. Measurements which were made indicate that the tip had receded a total of 1.27 mm from the original apex to the truncated surface. While there was a slight sand blasted appearance on the conical surface, there was no harsh pitting or cracks as seen on cathodes used with argon. A flattened conical tip was the extent of the metal loss, with no visible effects on the cylindrical surface. The perimeter of the melted region was smooth and free of dendrite formations that have appeared on cathodes used with storable propellants.[10] It should be emphasized, however, that these results represent only 28 hours of operation and that a full length life test would be needed to determine long term erosion effects

CONCLUDING REMARKS

A 30 kW class hydrogen arcjet was successfully operated using three different nozzle anode geometries. The arcjet was throttled over a wide range of power levels and flow rates with each nozzle to map and compare the effect of anode geometry on thruster performance. This process not only helped to find the optimum performance conditions, but demonstrated the versatility of a hydrogen arcjet with fixed geometry to adapt to off-design conditions without a gross penalty in performance.

A nozzle with a 2.54 mm ID constrictor was run at specific impulses ranging from 1026 s to 1411 s and thrust efficiencies ranging from 23% to 30.2 %. A nozzle with a 1.78 mm constrictor was run under similar circumstances and showed higher operating voltages and obtained thrust efficiencies typically 2 percentage points higher than the 2.54 mm constricted nozzle. The smaller constrictor had no difficulty enduring power levels as high as 30 kW, and it also showed improved stability at low flow rates. When it was operated at very high power, however, constrictor damage did occur. Therefore the 2.54 mm constrictor diameter may be better suited for peak power requirements in excess of 30 kW, and where it is less likely to be throttled to low flow rates.

A nozzle with a narrower 10 degree expansion angle was hindered by very high anode heat deposition which limited testing to low specific power levels. There was no observed performance advantage of a 10 degree expansion angle over the other geometries.

Post test examination of the nozzles showed arc damage which could be traced to specific regions of the test matrix where stability was poor or power levels were high. There were no indications of nozzle deterioration at moderate operating conditions.

Post test examination of the cathode indicated the conical tip had receded a total of 1.27mm over the course of 28 hours of operation, the majority of which had occurred with the first nozzle tested. Because of the limited duration of this testing, a full life test would be required to verify long term cathode erosion rates.

REFERENCES

1. Todd, J.P., "30 kW Arcjet Thruster Research," APL-TDR-64-58, Giannini Scientific Corp., Santa Ana, CA, Mar. 1964. (Avail. NTIS, AD-601534.)

2. John, R.R., "Thirty Kilowatt Plasmajet Rocket Engine Development," RAD-SR-64-168, Avco Corp., Wilmington, MA, 1964

3 Pivirotto, T.J., et al., "The Design and Operating Characteristics of a 30 KW Thermal Arcjet Engine for Space Propulsion." AIAA Paper 86-1508, June 1986.

4. Curran, F.M., and Haag, T.W., "An Extended Life and Performance Test of a Low-Power Arcjet," AIAA Paper 88-3106, July 1988

5 Haag, T.W., and Curran, F.M., "Arcjet Starting Reliability: A Multistart Test on Hydrogen/Nitrogen Mixtures," AIAA Paper 87-1061, May 1987, (NASA TM-89867).

6 Curran, F.M., Haag, T.H., and Raquet, J.F.,"Arcjet Cathode Phenomena," presented at the 1989 JANNAF Meeting, Cleveland, OH, May 1989, (NASA TM-102099).

7 Curran, F.M.,and Bullock, S.R., "Medium Power Hydrogen Arcjet Operation." AIAA Paper 91-2227, June 1991.

8 Sankovic, J.M., and Curran, F.M., "Arcjet Thermal Characteristics." AIAA Paper 91-2456, June 1991.

9. Jack, J.R., : Theoretical Performance of Propellants Suitable for Electrothermal Jet Engines. NASA TN D-682, 1961.

10 Pivirotto, T.J., and Deininger, W.D., "Analysis of a Used Pair of Arcjet Electrodes." Proceedings of SPIE, Volume 872, Propulsion, Jan. 1988, pp. 119- 162.

11. Goodfellow, K.D., "30 kW Ammonia Arcjet Throttling Test.", JPL D-8156, Jan. 1991

TABLE I. - DATA OBTAINED WITH NOZZLE A.

Flow, mg/s	Voltage, V	Current, A	Power, kW	Thrust, mN	Isp, s	Efficiency, %	P/ṁ, MJ/kg
122.8	0.0	0.0	0.00	303	251	100.0	0
30.9	96.3	69.6	6.70	311	1026	23.0	217
45.2	110.9	88.6	9.83	496	1117	27.2	217
45.2	103.4	109.3	11.30	511	1151	25.2	250
60.9	119.4	109.3	13.05	683	1145	29.0	214
60.9	120.3	108.4	13.05	687	1150	29.2	214
60.9	120.3	127.1	15.29	727	1218	28.0	251
60.9	119.8	135.8	16.26	753	1260	28.2	267
60.9	115.6	157.3	18.18	778	1302	27.0	299
60.9	119.5	153.0	18.28	780	1307	27.0	300
60.9	118.1	164.9	19.48	798	1336	26.5	320
71.6	125.7	194.7	24.48	1029	1377	28.1	321
76.2	126.8	128.4	16.28	872	1166	30.1	214
76.2	128.8	147.9	19.05	932	1246	29.5	250
76.2	128.4	167.6	21.52	982	1314	29.1	282
76.2	127.9	178.8	22.85	1008	1348	28.8	300
76.2	116.4	222.8	25.93	1045	1397	27.3	340
91.5	132.0	148.0	19.53	1047	1167	30.2	213
91.5	134.1	170.9	22.92	1131	1260	30.1	250
91.5	134.0	204.3	27.37	1209	1347	28.9	299
91.5	134.2	204.5	27.44	1216	1355	29.1	300
91.5	132.3	221.6	29.32	1245	1387	28.6	320
91.5	125.9	248.0	31.22	1267	1411	27.8	341
122.8	141.5	184.9	26.17	1382	1147	29.2	213
122.8	147.8	207.3	30.64	1495	1241	29.3	249
122.8	145.9	252.9	36.90	1625	1348	28.8	300
154.0	148.2	221.4	32.82	1714	1135	28.6	213
182.2	155.2	254.4	39.48	2030	1136	28.2	217

TABLE II. - DATA OBTAINED WITH NOZZLE B.

Flow, mg/s	Voltage, V	Current, A	Power, kW	Thrust, mN	Isp, s	Efficiency, %	P/ṁ, MJ/kg	Noz. Temp, C
91.5	0.0	0.0	0.00	255	250	100.0	0	
30.9	120.4	38.0	4.58	286	944	28.3	148	
45.2	135.6	49.7	6.74	450	1015	32.5	149	
45.2	134.1	67.3	9.02	496	1118	29.6	200	1032
45.2	121.1	93.2	11.30	533	1203	27.5	250	1145
60.9	145.3	62.5	9.08	613	1027	33.3	149	
60.9	144.9	84.0	12.20	689	1154	31.4	200	1096
60.9	141.9	107.4	15.24	754	1264	30.3	250	1486
60.9	142.4	107.3	15.30	748	1253	29.6	251	1189
60.9	139.9	130.4	18.24	804	1347	28.8	300	1625
76.2	152.0	75.6	11.50	770	1030	33.1	151	
76.2	150.9	101.0	15.20	883	1181	33.1	200	1247
76.2	150.4	126.5	19.03	965	1291	31.7	250	1544
76.2	150.5	126.9	19.10	967	1294	31.7	251	1384
76.2	149.0	153.6	22.90	1025	1371	29.8	300	1326
76.2	147.8	175.4	25.92	1081	1446	29.3	340	1325
91.5	160.4	85.3	13.68	938	1045	34.4	149	
91.5	159.7	114.8	18.30	1064	1185	33.2	200	1259
91.5	158.7	144.1	22.90	1170	1303	32.2	250	1422
91.5	153.5	149.0	22.87	1152	1283	31.3	250	1789
91.5	155.0	177.4	27.50	1252	1395	30.8	300	
91.5	154.5	177.9	27.49	1250	1392	30.7	300	1623
91.5	155.0	200.9	31.14	1310	1460	29.8	340	2061
122.8	172.2	107.1	18.44	1238	1028	33.1	150	
122.8	170.8	144.2	24.60	1405	1166	32.1	200	1300
122.8	168.7	182.2	30.70	1545	1282	32.1	250	1462
122.8	161.0	260.5	41.94	1761	1461	29.8	341	2108
147.4	181.4	121.1	22.11	1478	1022	32.8	150	
148.0	179.8	166.2	29.90	1682	1158	31.4	202	1347

TABLE III. - DATA OBTAINED WITH NOZZLE C.

Flow, mg/s	Voltage, V	Current, A	Power, kW	Thrust, mN	Isp, s	Efficiency, %	P/ṁ, MJ/kg	Noz. Temp, C
91.5	0.0	0.0	0.00	224	250	100.0	0	
45.2	91.3	74.1	6.77	393	886	24.7	150	1599
60.9	102.8	58.4	60.03	477	798	30.1	99	
60.9	95.2	95.5	9.09	555	929	27.7	149	1736
60.9	97.2	125.0	12.15	604	1012	24.3	200	2142
76.2	106.0	107.6	11.41	726	971	29.6	150	1790
76.2	107.3	107.6	11.55	731	978	29.7	152	1869
76.2	103.7	146.8	15.22	791	1058	26.5	200	2060
91.5	109.8	166.5	18.28	976	1088	28.0	200	2114
91.5	114.7	119.5	13.71	894	996	31.2	150	1846
107.2	116.6	165.4	19.29	1117	1062	29.6	180	2000
122.8	120.4	153.0	18.42	1220	1012	32.2	150	1884
122.8	113.6	162.0	18.40	1223	1015	32.4	150	1938
122.8	118.8	207.3	24.63	1350	1120	29.6	200	2162
138.4	123.9	197.5	24.47	1481	1091	31.8	177	1705
154.0	128.2	179.7	23.04	153	1017	32.5	150	1965
154.0	126.5	243.7	30.83	1704	1128	30.1	200	2313
182.2	134.5	202.9	27.29	1811	1013	32.2	150	1946
182.2	128.6	212.1	27.28	1814	1015	32.4	150	1936
213.0	141.3	226.2	31.96	2098	1004	31.6	150	1941

Constrictor diameter = 2.54 mm
Constrictor length = 5.08 mm
Expansion angle = 20 deg
Exit diameter = 24.3 mm

(a) Geometry of nozzle A.

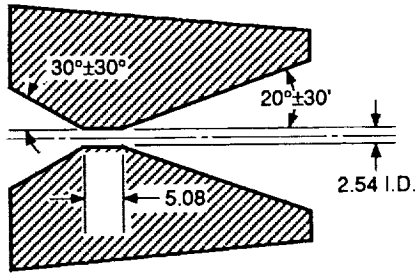

Nozzle A

Constrictor diameter = 1.78 mm
Constrictor length = 3.56 mm
Expansion angle = 20 deg
Exit diameter = 29.0 mm

(b) Geometry of nozzle B.

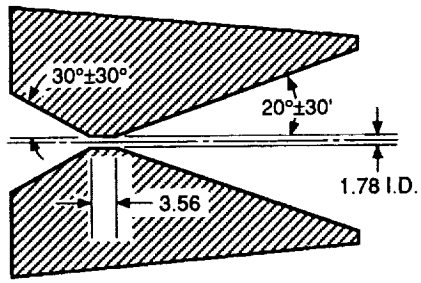

Nozzle B

Constrictor diameter = 2.54 mm
Constrictor length = 0.71 mm
Expansion angle = 10 deg
Exit diameter = 24.3 mm

(c) Geometry of nozzle C.

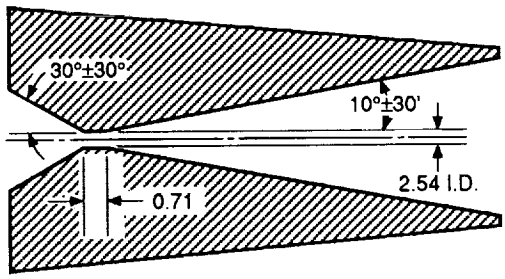

Nozzle C

Figure 1.—Nozzle geometry used in hydrogen arcjet performance test.

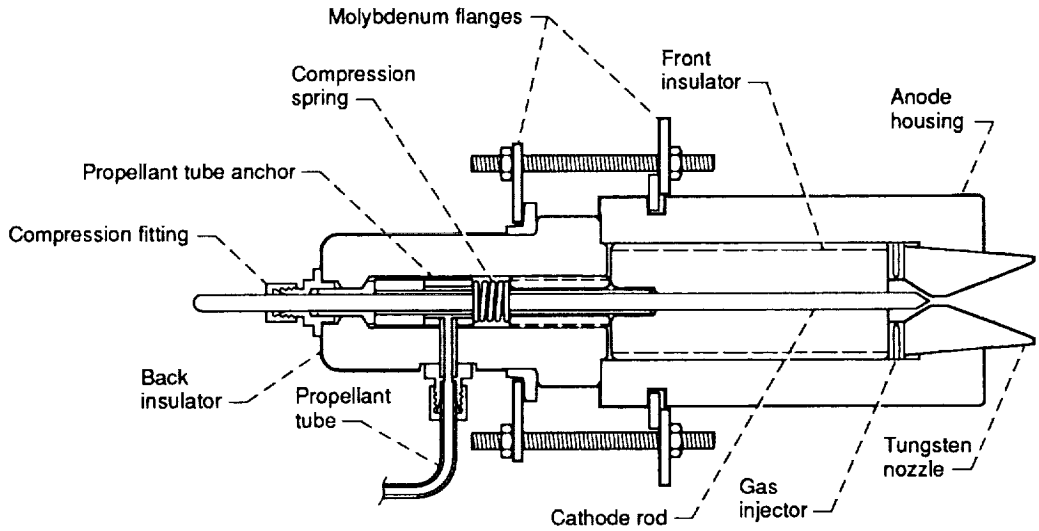

Figure 2.—Schematic of 30 kW hydrogen arcjet thruster.

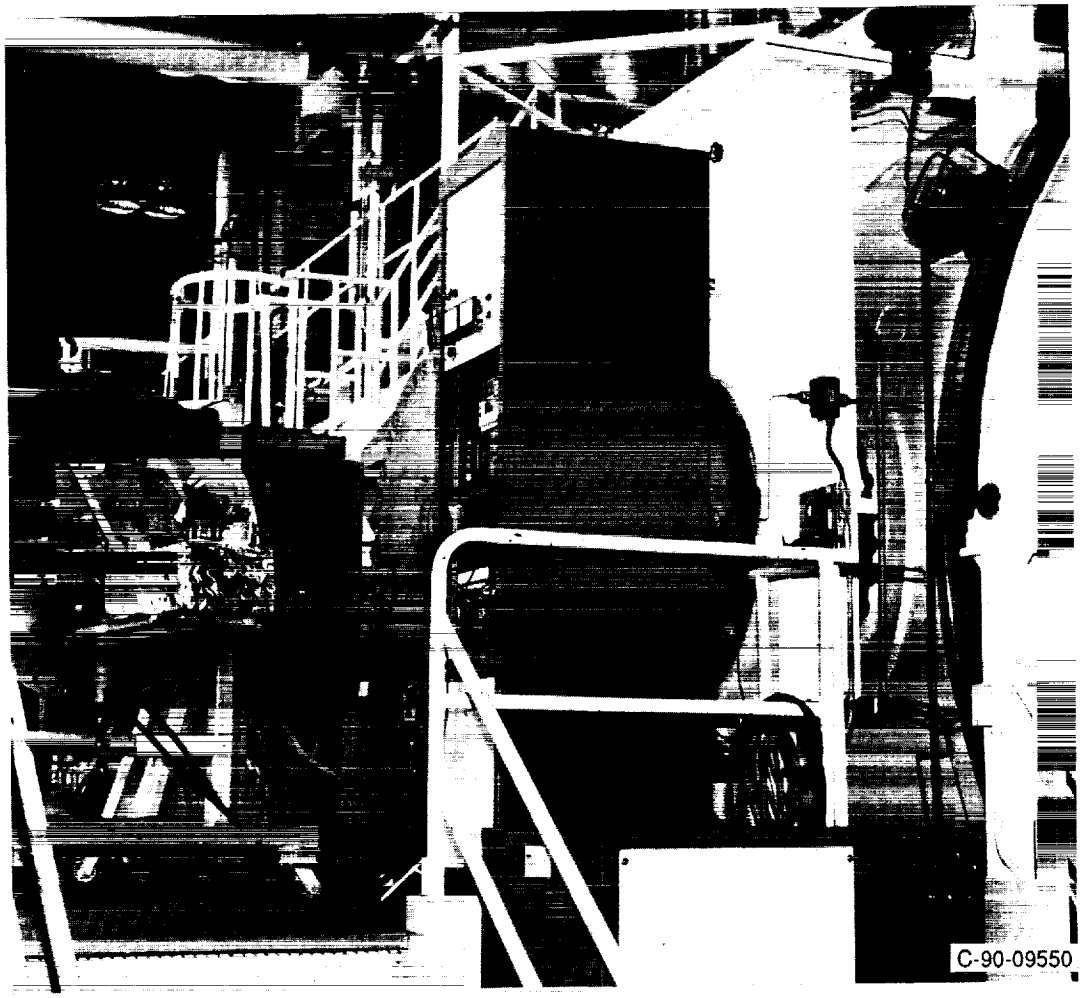

Figure 3.—Photograph of thrust stand, 0.9 m test port, and main vacuum tank.

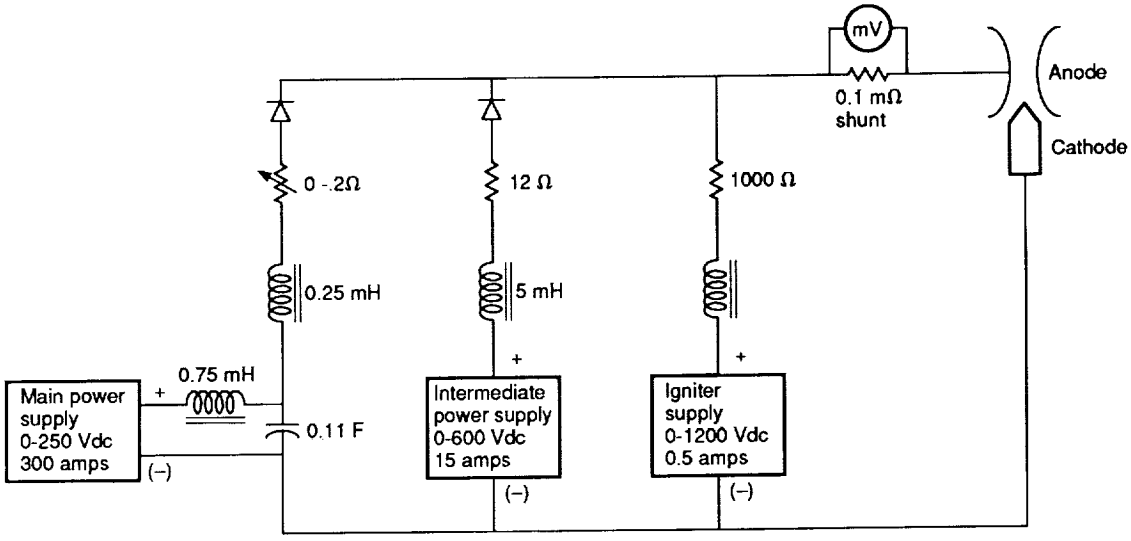

Figure 4.—Arcjet power supply schematic.

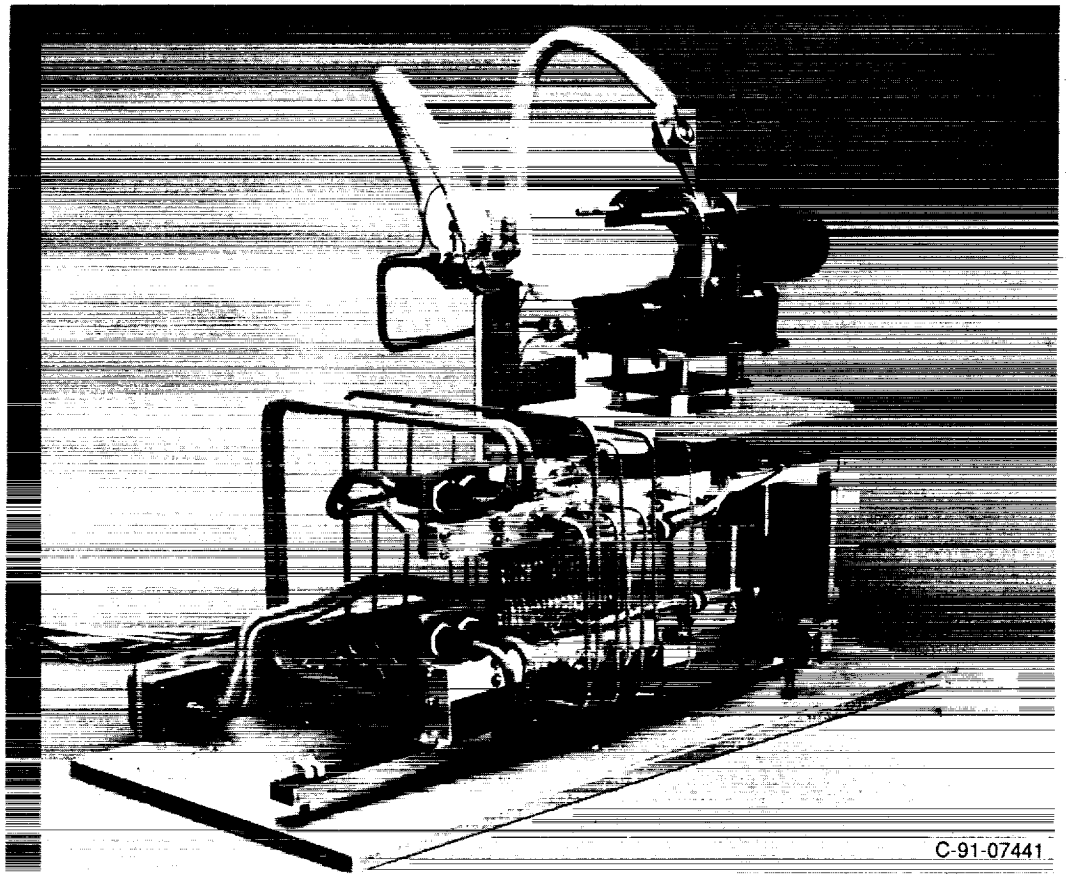

Figure 5.—Rear view of thrust stand with water cooled enclosure removed.

Figure 6.—Photograph of 30 kW hydrogen arcjet at thermal equilibrium. Langmuir probe visible in exhaust plume.

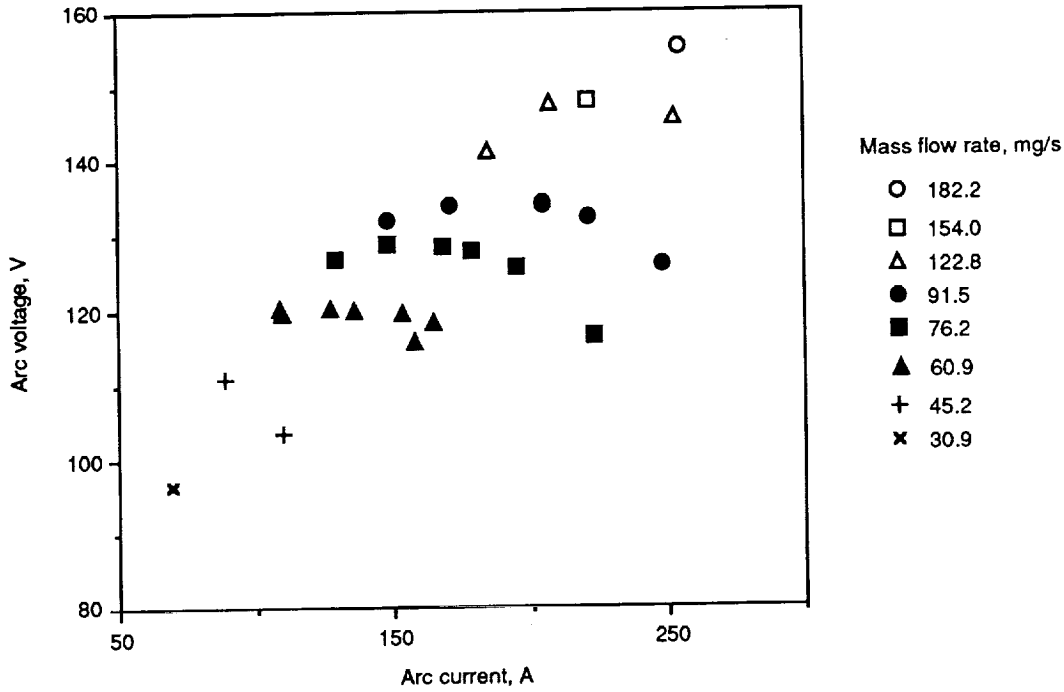

Figure 7.—Voltage-current characteristics of nozzle A for various propellant flow rates.

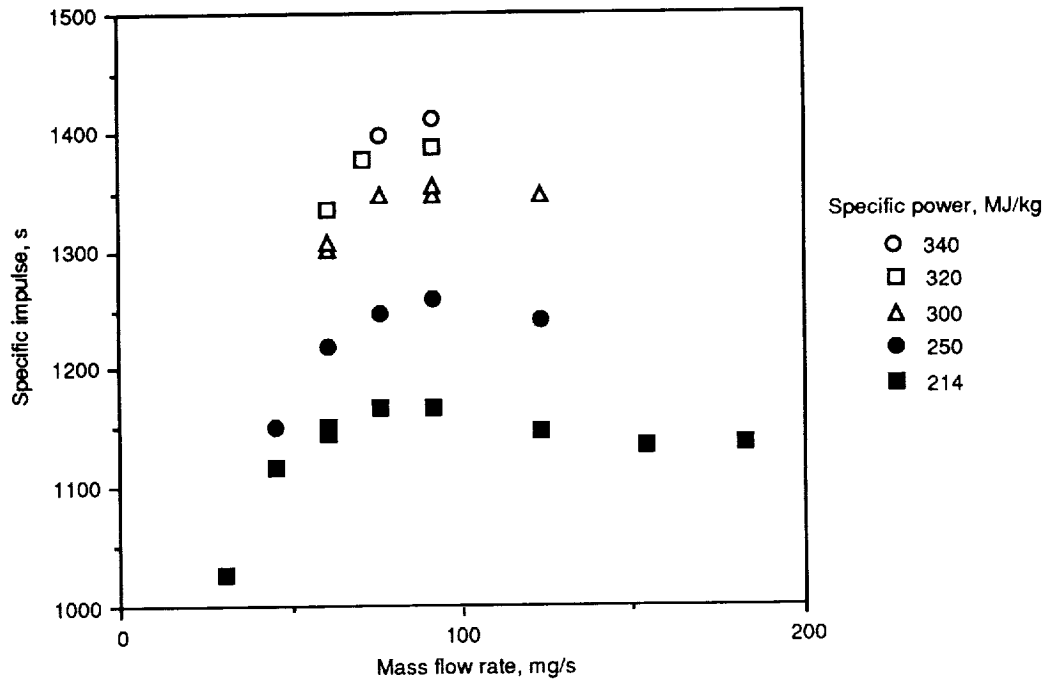

Figure 8.—Specific impulse of nozzle A as a function of propellant flow rate for various specific power levels.

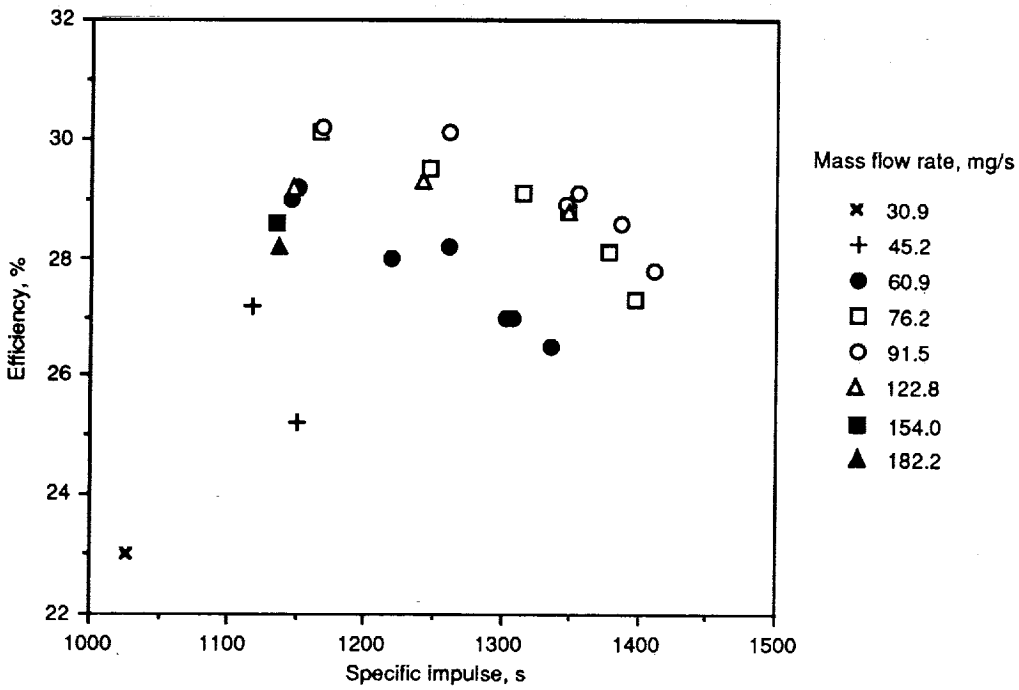

Figure 9.—Thrust efficiency of nozzle A as a function of specific impulse for various propellant flow rates.

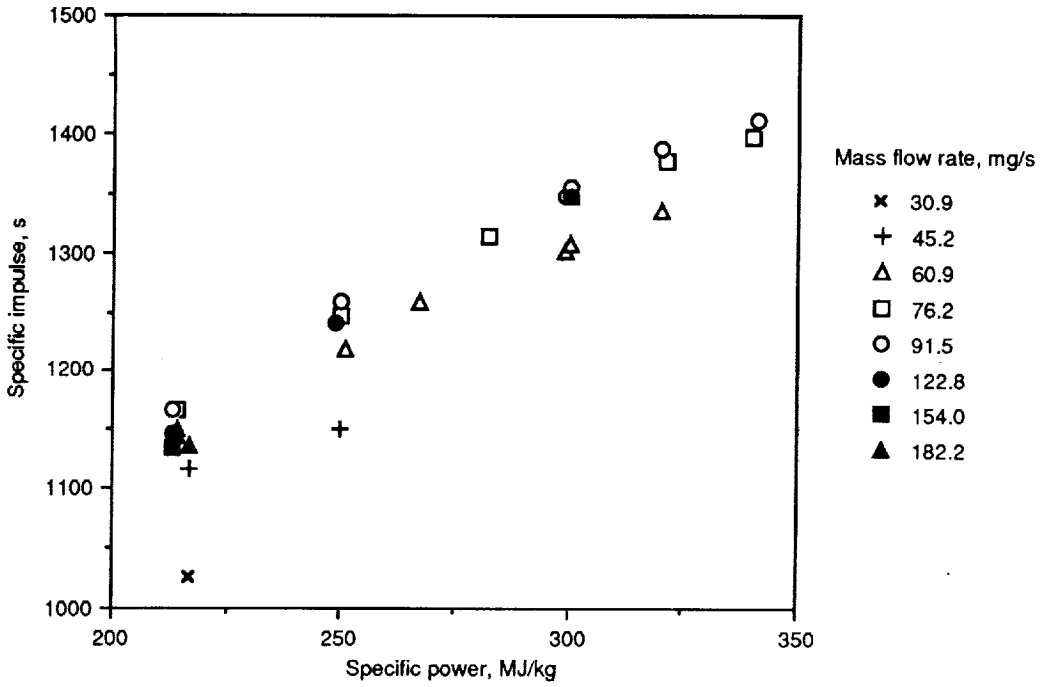

Figure 10.—Specific impulse of nozzle A as a function of specific power for various propellant flow rates.

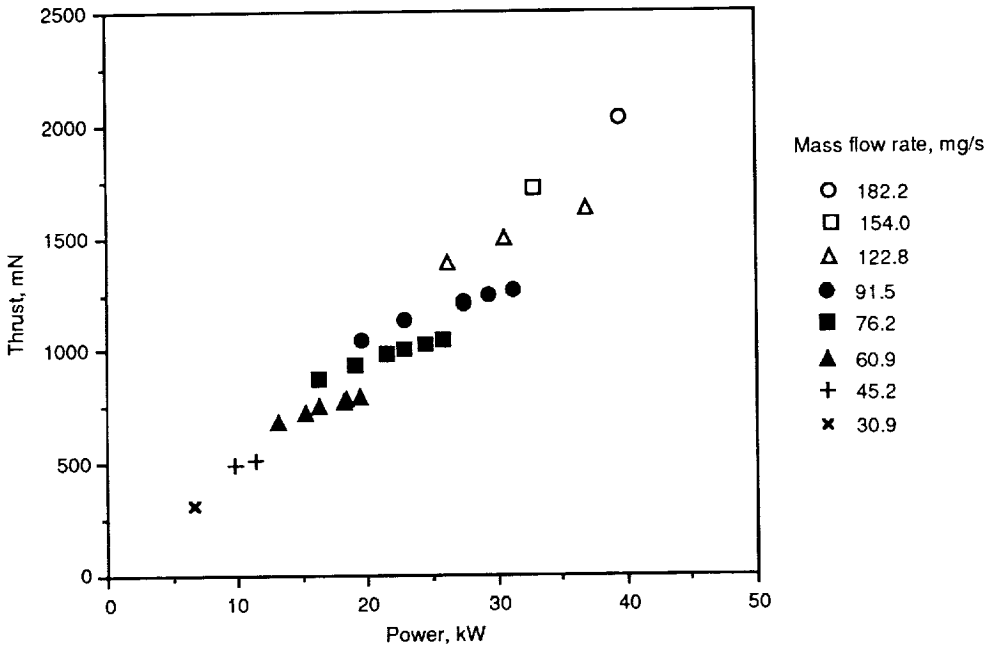

Figure 11.—Thrust of nozzle as a function of power level for various propellant flow rates.

Figure 12.—Photograph of diverging side of nozzle A showing arc damage in constrictor region.

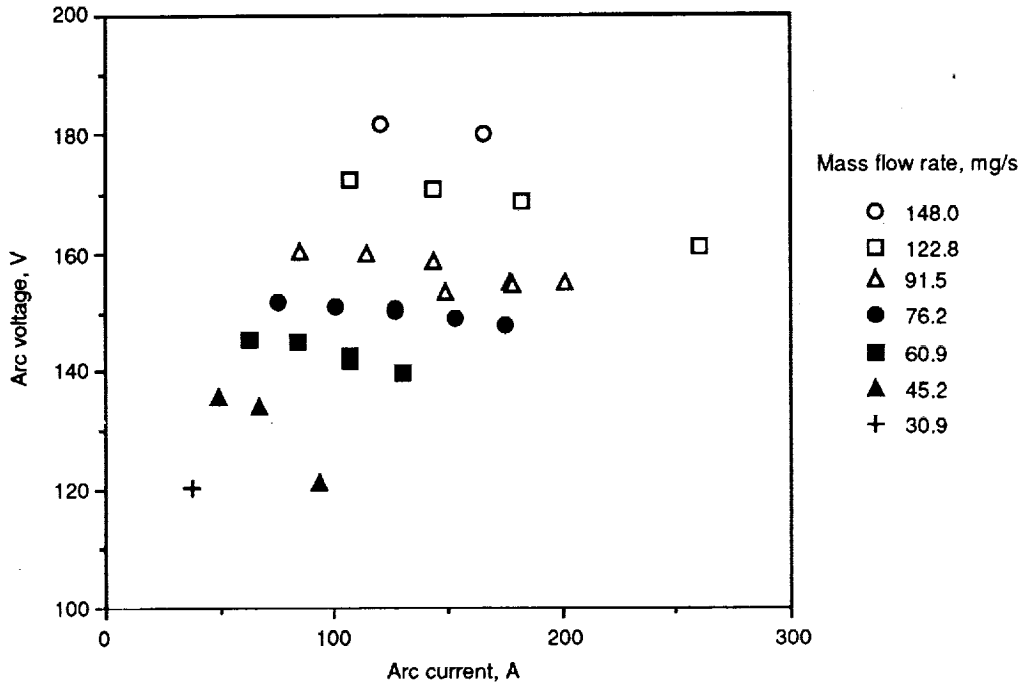

Figure 13.—Voltage-current characteristics of nozzle B for various propellant flow rates.

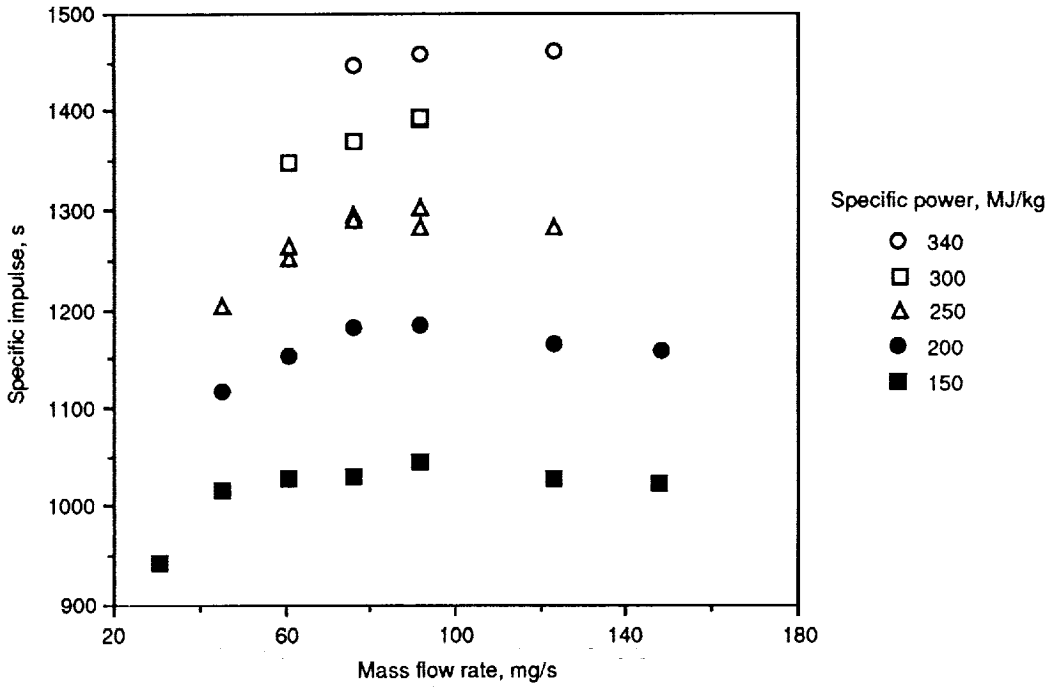

Figure 14.—Specific impulse of nozzle B as a function of propellant flow rate for various specific power levels.

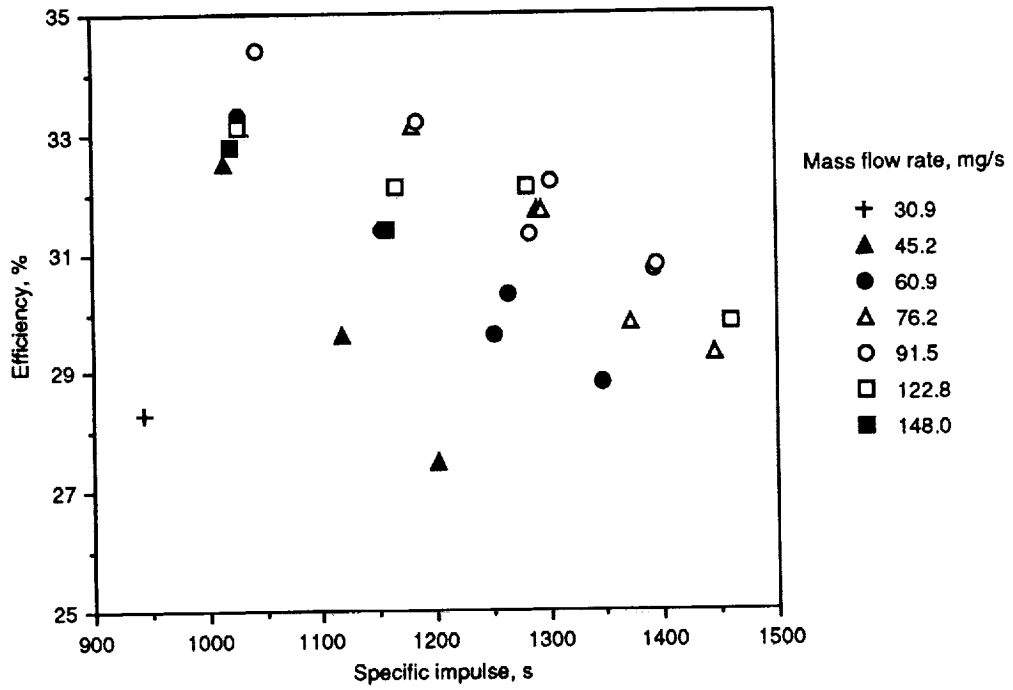

Figure 15.—Thrust efficiency of nozzle B as a function of specific impulse for various propellant flow rates.

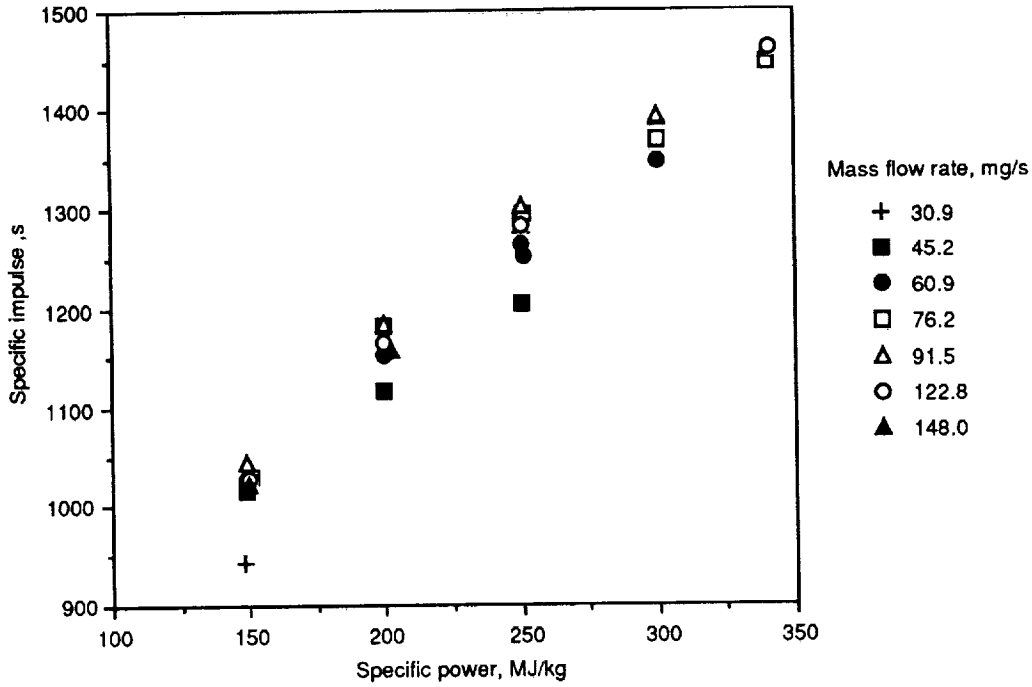

Figure 16.—Specific impulse of nozzle B as a function of specific power for various propellant flow rates.

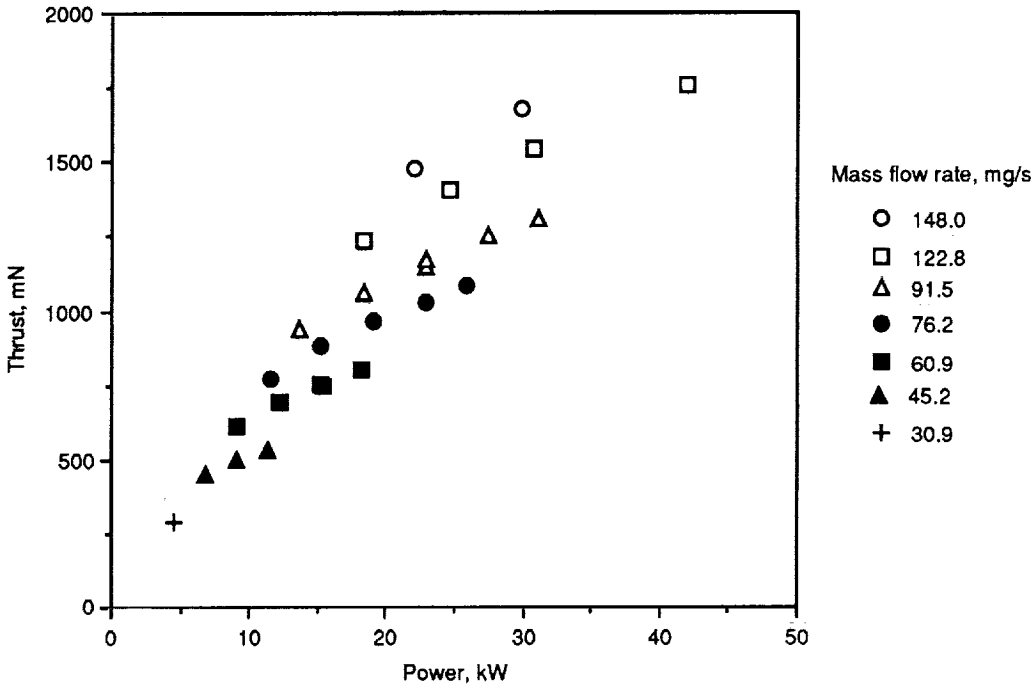

Figure 17.—Thrust of nozzle B as a function of power level for various propellant flow rates.

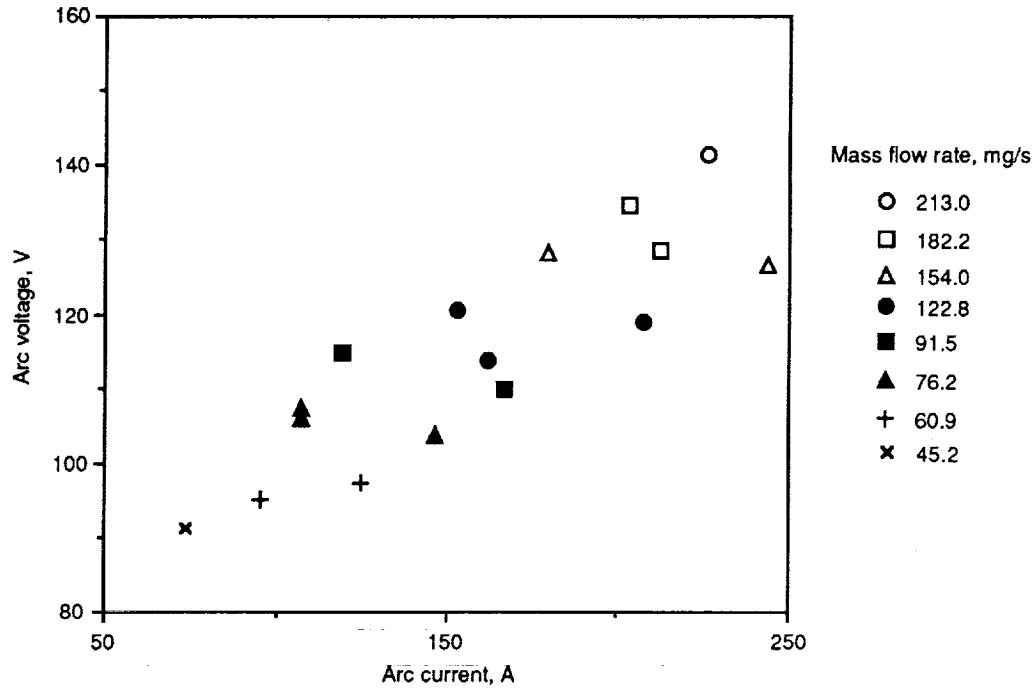

Figure 18.—Voltage-current characteristics of nozzle C for various propellant flow rates.

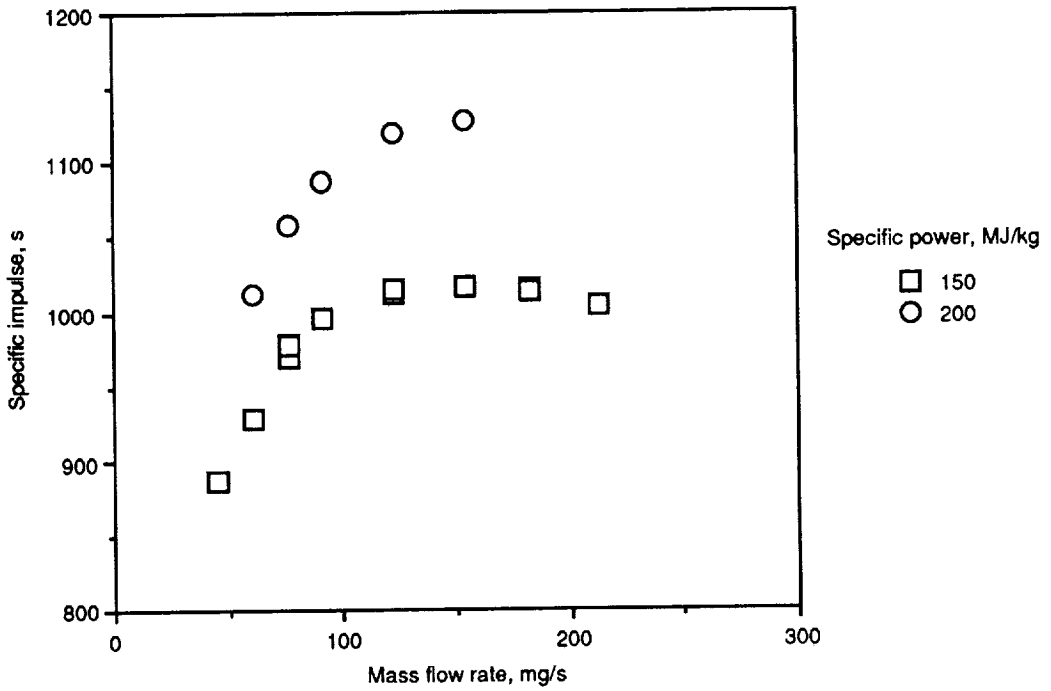

Figure 19.—Specific impulse of nozzle C as a function of propellant flow rate for various specific power levels.

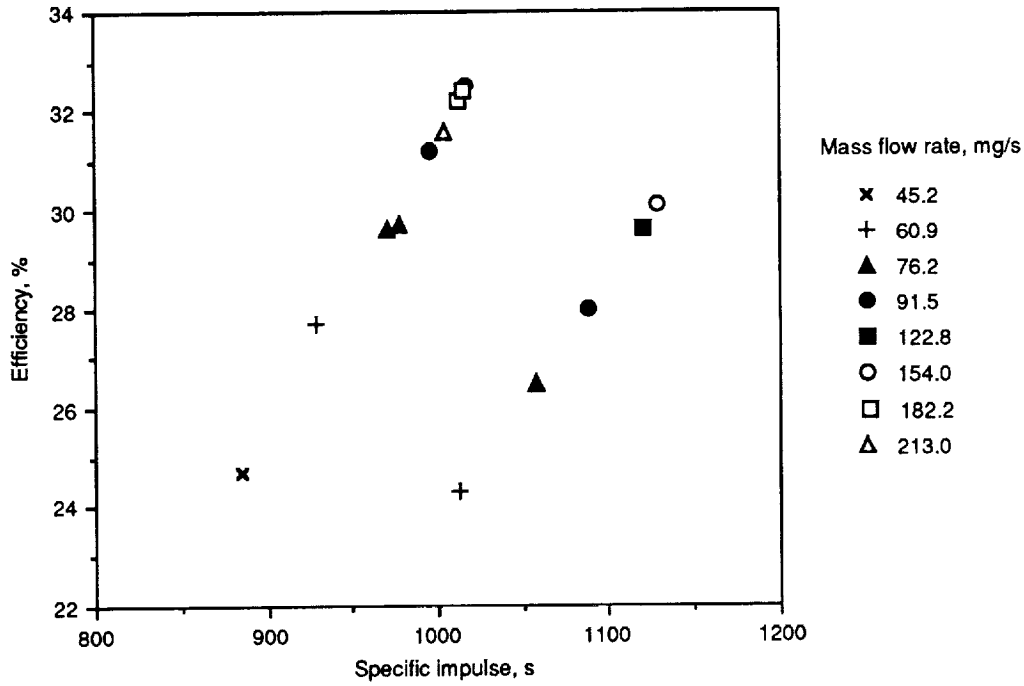

Figure 20.—Thrust efficiency of nozzle C as a function of specific impulse for various propellant flow rates.

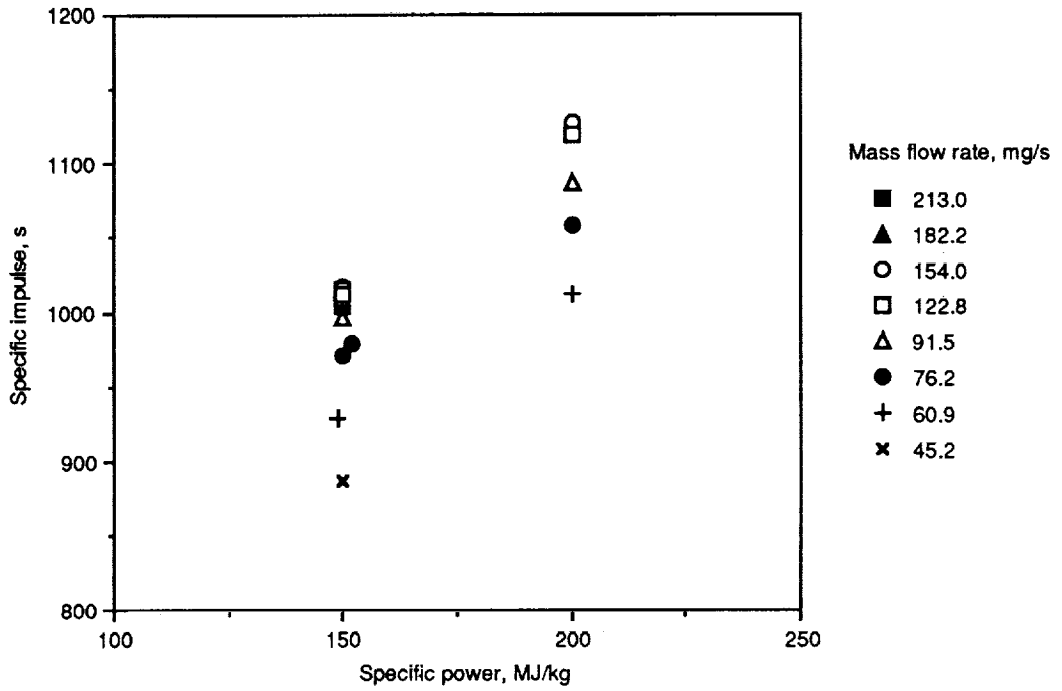

Figure 21.—Specific impulse of nozzle C as a function of specific power for various propellant flow rates.

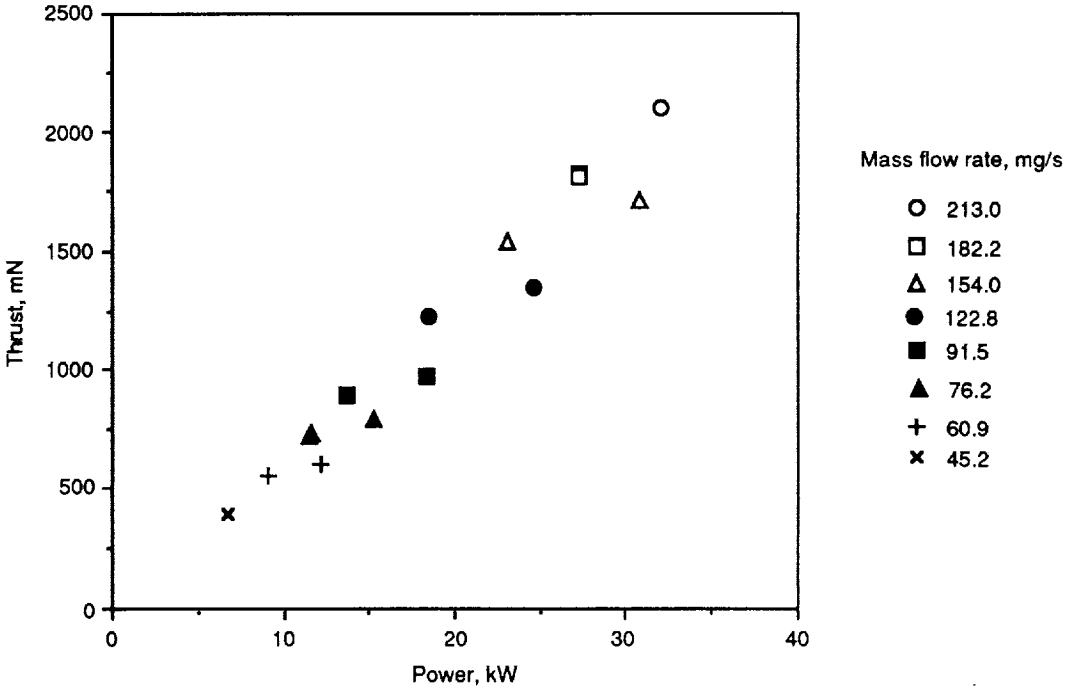

Figure 22.—Thrust of nozzle C as a function of power level for various propellant flow rates.

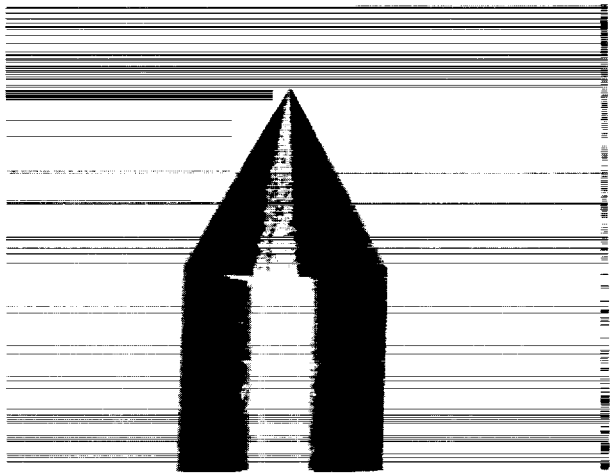

(a) Photograph of 6.35 mm O.D. cathode with newly machined finish. Conical tip with 30 deg half angle.

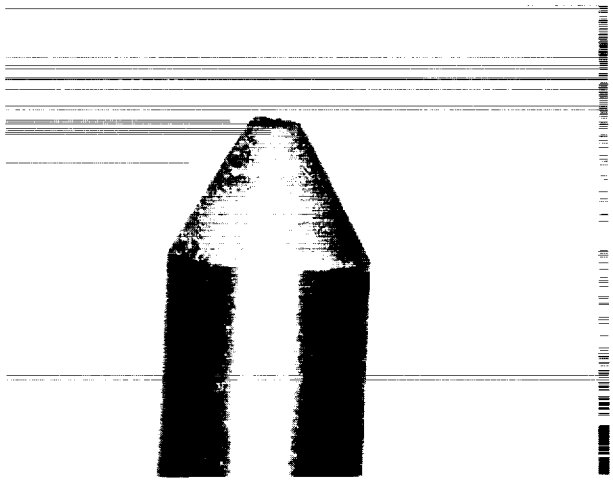

(b) Photograph of arcjet cathode after use with Nozzles A, B, and C. Represents 141 starts and approximately 28 hrs of operation using H_2. Tip receded a total of 1.27 mm.

Figure 23.—Photographs of cathode tip before and after testing.

REPORT DOCUMENTATION PAGE

Form Approved
OMB No. 0704-0188

1. AGENCY USE ONLY (*Leave blank*)	2. REPORT DATE	3. REPORT TYPE AND DATES COVERED
		Technical Memorandum

4. TITLE AND SUBTITLE

High-Power Hydrogen Arcjet Performance

5. FUNDING NUMBERS

WU-506-42-31

6. AUTHOR(S)

Thomas W. Haag and Francis M. Curran

7. PERFORMING ORGANIZATION NAME(S) AND ADDRESS(ES)

National Aeronautics and Space Administration
Lewis Research Center
Cleveland, Ohio 44135-3191

8. PERFORMING ORGANIZATION REPORT NUMBER

E-6418

9. SPONSORING/MONITORING AGENCY NAMES(S) AND ADDRESS(ES)

National Aeronautics and Space Administration
Washington, D.C. 20546-0001

10. SPONSORING/MONITORING AGENCY REPORT NUMBER

NASA TM-105143
AIAA-91-2226

11. SUPPLEMENTARY NOTES

Prepared for the 27th Joint Propulsion Conference cosponsored by AIAA, SAE, ASME, and ASEE, Sacramento, California, June 24-27, 1991. Responsible person, Thomas W. Haag, (216) 433-2709.

12a. DISTRIBUTION/AVAILABILITY STATEMENT

Unclassified - Unlimited
Subject Category 20

12b. DISTRIBUTION CODE

13. ABSTRACT (*Maximum 200 words*)

A hydrogen arcjet was operated at power levels ranging from 5 to 30 kW with three different nozzle geometries. Test results using all three nozzle geometries are reported and include variations of specific impulse with flow rate, and thrust with power. Geometric variables investigated included constrictor diameter, length, and diverging exit angle. The nozzle with a constrictor diameter of 1.78 mm and divergence angle of 20° was found to give the highest performance. A specific impulse of 1460 s was attained with this nozzle at a thrust efficiency of 29.8%. The best efficiency measured was 34.4% at a specific impulse of 1045 s. Post test examination of the cathode showed erosion after 28 hours of operation to be small, and limited to the conical tip where steady state arc attachment occurred. Each nozzle was tested to destruction.

14. SUBJECT TERMS	15. NUMBER OF PAGES
Arcjet engines; Electric propulsion; Spacecraft propulsion	22
	16. PRICE CODE A03

17. SECURITY CLASSIFICATION OF REPORT	18. SECURITY CLASSIFICATION OF THIS PAGE	19. SECURITY CLASSIFICATION OF ABSTRACT	20. LIMITATION OF ABSTRACT
Unclassified	Unclassified	Unclassified	